第33卷 第4期 焊 接 学 报 Vol. 33 No. 4
2012年4月 TRANSACTIONS OF THE CHINA WELDING INSTITUTION April 2012

焊接机器人虚拟样机轨迹模拟和运动仿真分析

王 玉[1]， 王旗华[2]， 赵建光[3]， 张兆隆[1]
(1. 河北机电职业技术学院 机械工程系，邢台 054048; 2. 四川大学 制造科学与工程学院，成都 610065;
3. 河北机电职业技术学院 电气工程系，邢台 054048)

摘 要: 根据焊接机器人的结构特点，对其进行了模型简化，在对机器人进行正向运动学分析的基础上，运用 Denavit-Hartenberg(D-H) 矩阵法，求解出焊接机器人末端位姿的数学模型，完成了焊接机器人空间位姿的描述; 运用 ADAMS 软件，建立了焊接机器人的虚拟样机模型，仿真得出了模型的末端轨迹，并与数学模型求解结果进行对比，验证了数学模型的准确性与可靠性; 对其进行运动仿真分析，测量并研究了机器人各关节运动学参数的变化情况，为后续焊接机器人的设计和制造提供了依据，对于精确确定焊枪工作位置、确保焊接质量、降低产品废品率有重要意义.

关键词: 焊接机器人; 虚拟样机; 自由度; ADAMS; 运动仿真
中图分类号: TP18 **文献标识码:** A **文章编号:** 0253-360X(2012)04-0109-04

王 玉

0 序 言

焊接加工一方面要求工人有熟练的操作技能、丰富的实践经验、稳定的焊接水平; 另一方面，工作的劳动条件差、烟尘多、热辐射大、危险性高. 焊接机器人是在焊接生产中代替工人从事焊接工作的工业机器人. 利用焊接机器人代替人工焊接，可减轻工人的劳动强度，保证焊接质量和提高焊接效率. 因此焊接机器人广泛用于汽车零部件制造、造船、石油、化工及航天中. 能否高质量地完成焊接工作，焊接机器人的末端位姿是否到位、机械手的运行是否平稳等是关键. 所以设计中、制造前对焊接机器人进行轨迹模拟及运动仿真分析尤为重要.

为保证焊接质量，研制时需对其进行轨迹设计和运动学分析，即研究机械手的运动轨迹和各关节的速度、加速度等. 焊接机器人是多自由度、多连杆的串联式空间机构，其运动学和动力学问题复杂，人工计算难度很大. 若将焊接机器人作为仿真对象，运用造型和仿真软件生成三维和仿真模型，模拟机器人的工作过程，仿真其运动轨迹、速度和加速度，可有效避免工作过程中出现的问题. 文中建立了焊接机器人末端位姿数学和仿真模型，进行轨迹和运动仿真分析，取得了良好的结果.

收稿日期: 2011-03-02

1 焊接机器人的分析模型及自由度

文中系统的焊接机器人属于关节式机器人，是由一系列关节连接起来的连杆所组成的，用一个开环关节链来建模，将其模型化为由 6 个杆件用 5 个以驱动器驱动的转动关节，串联而成的开环系统，即躯干与肩、肩与手臂、手臂与手腕、手腕与机械手、底座与躯干均以转动副相连. 开链的一端躯干固定在基座上，另一端机械手是自由的安装着焊枪以完成焊接作业. 关节的相对运动导致杆件的运动，使焊枪定位于所需方位[1].

由自由度计算公式[2]为

$$M = 6(n - g - 1) + \sum_{i=1}^{g} f_i \qquad (1)$$

式中: n 为活动构件数目; g 为运动副数目; f_i 为第 i 个运动副的相对自由度数.

得该机器人的自由度为

$$M = 6 \times (6 - 5 - 1) + 5 = 5$$

所以建模时在 5 个转动副位置添加 5 个驱动.

2 焊接机器人末端位姿数学模型

机器人正向运动学是指由机器人各关节角(θ_0, θ_1, $\cdots$, θ_n)，计算机械手上某一点(即焊枪)的位置和方向，主要解决机器人运动学方程的建立及机械手姿态的求解问题，其方法为求联系附体坐标系和参

考坐标系的变换矩阵. 对每个杆件沿关节轴建立一个附体坐标系,如图 1 用 D-H (Denavit-Hartenberg) 矩阵法,附体坐标系相对于参考坐标系的转动和移动 4 ×4 齐次变换矩阵来描述.

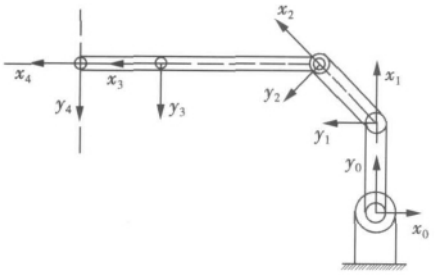

图 1 焊接机器人坐标系

Fig. 1 Coordinate systems of welding robot

分别用 A_1^0,A_2^1,A_3^2,A_4^3,A_5^4 矩阵表示躯干坐标系相对于基座坐标系、肩坐标系相对于躯干坐标系、手臂坐标系相对于肩坐标系、腕坐标系相对于手臂坐标系、机械手坐标系相对于腕坐标系的位姿,则该 5 连杆(躯干、肩、臂、腕、机械手) 机器人手部坐标系相对于固定参考系下的位姿 T_5^0,等于从固定参考系到手部坐标系的各连杆坐标系之间的变换矩阵的连乘,即

$$T_5^0 = A_1^0 A_2^1 A_3^2 A_4^3 A_5^4 \tag{2}$$

则

$$T_5^0 = \begin{bmatrix} n_x & o_x & a_x & p_x \\ n_y & o_y & a_y & p_y \\ n_z & o_z & a_z & p_z \\ 0 & 0 & 0 & 1 \end{bmatrix} \tag{3}$$

图 1 所示 5 自由度焊接机器人 D-H 参数见表 1.

表 1 5 自由度焊接机器人 D-H 参数

Table 1 D-H table of 5-DOF welding robot

序列 i	连杆扭转角 α_j/(°)	连杆长度 l_i/mm	连杆偏距 d_i/mm	转角 θ_i/(°)
1	0	l_1	0	θ_1
2	0	l_2	0	θ_2
3	0	l_3	0	θ_3
4	0	l_4	0	θ_4
5	0	l_5	0	θ_5

建立相邻连杆坐标系间的齐次变换矩阵得

$$A_i^{i-1} = \begin{bmatrix} \cos\theta_i & -\sin\theta_i & 0 & l_i\cos\theta_i \\ \sin\theta_i & \cos\theta_i & 0 & l_i\cos\theta_i \\ 0 & 0 & 1 & 0 \\ 0 & 0 & 0 & 1 \end{bmatrix}$$

则

$$T_5^0 = \begin{bmatrix} \cos\theta_{12345} & -\sin\theta_{12345} & 0 & l_1\cos\theta_1 + l_2\cos\theta_{12} + l_3\cos\theta_{123} + l_4\cos\theta_{1234} + l_5\cos\theta_{12345} \\ \sin\theta_{12345} & \cos\theta_{12345} & 0 & l_1\sin\theta_1 + l_2\sin\theta_{12} + l_3\sin\theta_{123} + l_4\sin\theta_{1234} + l_5\sin\theta_{12345} \\ 0 & 0 & 1 & 0 \\ 0 & 0 & 0 & 1 \end{bmatrix} \tag{4}$$

式中: θ_i 为连杆相对于相邻连杆的转角,$\theta_{ij} = \theta_i + \theta_j$,$\cos\theta_{ij} = \cos(\theta_i + \theta_j)$,$\sin\theta_{ij} = \sin(\theta_i + \theta_j)$.

由式(3) 和式(4) 得

$$\begin{aligned}
n_x &= \cos(\theta_1 + \theta_2 + \theta_3 + \theta_4 + \theta_5) \\
n_y &= \sin(\theta_1 + \theta_2 + \theta_3 + \theta_4 + \theta_5) \\
o_x &= -\sin(\theta_1 + \theta_2 + \theta_3 + \theta_4 + \theta_5) \\
o_y &= \cos(\theta_1 + \theta_2 + \theta_3 + \theta_4 + \theta_5) \\
p_x &= l_1\cos\theta_1 + l_2\cos(\theta_1 + \theta_2) + l_3\cos(\theta_1 + \theta_2 + \theta_3) \\
&\quad + l_4\cos(\theta_1 + \theta_2 + \theta_3 + \theta_4) + l_5\cos(\theta_1 + \theta_2 + \theta_3 + \theta_4 + \theta_5) \\
p_y &= l_1\sin\theta_1 + l_2\sin(\theta_1 + \theta_2) + l_3\sin(\theta_1 + \theta_2 + \theta_3) + \\
&\quad l_4\sin(\theta_1 + \theta_2 + \theta_3 + \theta_4) + l_5\sin(\theta_1 + \theta_2 + \theta_3 + \theta_4 + \theta_5)
\end{aligned}$$

用 $f = (x, y, \phi)$ 表示机器人末端位姿,则

$$\left.\begin{aligned}
x &= l_1\cos\theta_1 + l_2\cos\theta_{12} + l_3\cos\theta_{123} + l_4\cos\theta_{1234} + l_5\cos\theta_{12345} \\
y &= l_1\sin\theta_1 + l_2\sin\theta_{12} + l_3\sin\theta_{123} + l_4\sin\theta_{1234} + l_5\sin\theta_{12345} \\
\phi &= \theta_{12345}
\end{aligned}\right\} \tag{5}$$

3 焊接机器人仿真建模

虚拟样机技术是一种基于产品计算机仿真模型的数字化设计方法,最常用的应用软件为美国 MSC 公司的 ADAMS(automatic dynamic analysis of mechanical system) 软件[3] . ADAMS 软件可以快速方便地建立机械系统的仿真模型,并将模型参数化,然后在模型上施加驱动,运行仿真结果,进行运动学和动力学分析,输出位移、速度、加速度和作用力曲线. 用于预测机械系统的性能、运动轨迹、碰撞检测等[4] .

该焊接机器人由底座、躯干、肩、手臂、手腕和机械手 6 部分构成[5] . 焊接机器人的各关节均为转动关节,所以除在机座与地基联接处施加固结副外,躯干与肩、肩与手臂、手臂与手腕、手腕与机械手、躯干与机座联接处均施加转动副,对其进行约束,并在躯

干与肩、肩与手臂、手臂与手腕、手腕与机械手、躯干与机座联接处施加驱动 MOTION_1,MOTION_2,MOTION_3,MOTION_4、MOTION_5.

在 ADAMS 环境下的焊接机器人虚拟样机模型如图 2 所示.

图 2　焊接机器人末端轨迹

Fig. 2　Tip trajectory of welding robot

4　焊接机器人运动仿真

建模完成,进行仿真,绘制机械手末端在仿真过程中的运动轨迹. 黑色的曲线即为机械手末端点的运动轨迹. 图 2 表明了机械人按规划的轨迹执行作业的仿真过程. 观察可知在仿真的过程中,机器人运行连续、平稳,无因错误导致的停顿现象.

由上述曲线可得出结论,机器人能根据规划路径到达规划点,过程中运动平稳、无剧烈的抖动现象,加速度小且加速度无突变、运转时冲击不大.

5　焊接机器人运动分析

机械手的位移、速度、加速度,各关节角位移、角速度、角加速度是保证焊缝质量的重要参数,也是焊接机器人运动学研究的重要参数. 用 ADAMS 测量功能,测量仿真过程中这些重要参数的变化情况,获得机器人各关节的运动特性曲线,便于及时发现设计中的不合理问题.

5.1　机械手位移与速度及加速度测量

在后处理(postprocessor) 程序窗口中,绘制机械手 x,y 方向的位移、速度、加速度曲线,如图 3 ~ 图 5 所示.

由图 3 可知,机械手 x,y 方向的位移曲线光滑连续,没有尖点,表明机器人机械手在工作过程中,动作符合焊条运动要求; 由图 4 和图 5 可知机械手

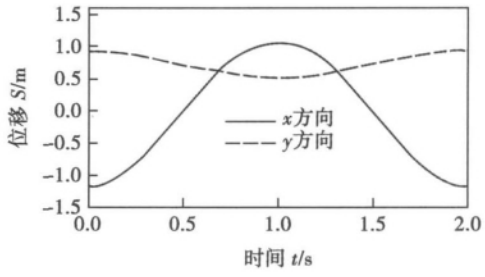

图 3　机械手 x 和 y 方向的位移曲线

Fig. 3　Curve x, y direction of displacement for manipulator

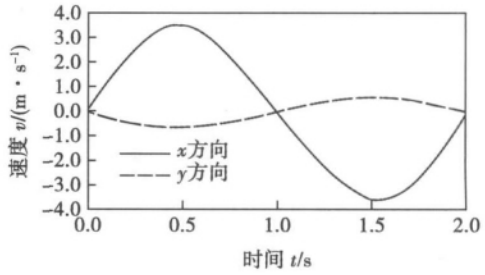

图 4　机械手 x 和 y 方向的速度曲线

Fig. 4　Curve x, y direction of velocity for manipulator

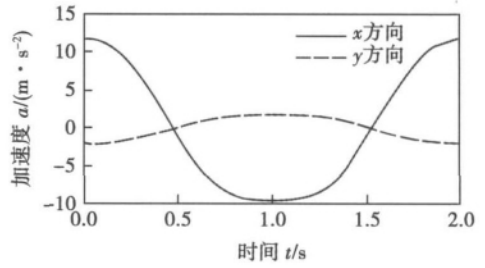

图 5　机械手 x 和 y 方向的加速度曲线

Fig. 5　Curve x, y direction of acceleration for manipulator

x,y 方向的速度、加速度曲线光滑连续、没有突变,表明机械手在工作过程中,运动平稳,无较大冲击,可以保证焊接质量.

5.2　关节角位移与角速度及角加速度测量

测量各关节的关节角位移、角速度、角加速度,仿真过程中通过 measure 窗口动态观察关节角位移的变化情况,以肩与臂关节为例,其角位移曲线如图 6所示、速度、加速度曲线如图 7 所示.

由图 6 和图 7 可知,整个运动过程中,机器人肩与臂、臂与腕各关节角度、角速度、角加速度变化连续,无剧烈抖动现象,表明运动平稳、无较大冲击,这就减少了机器人零件磨损,延长了机器人的使用寿命. 图 8 为躯干绕基座转动的角位移曲线,由图 8 可知,躯干转动的角位移曲线为一次函数斜直线,说

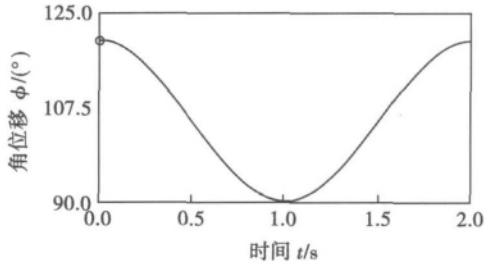

图 6 肩与臂关节角位移曲线

Fig. 6 Curve of angular displacement for shoulder and arm joint

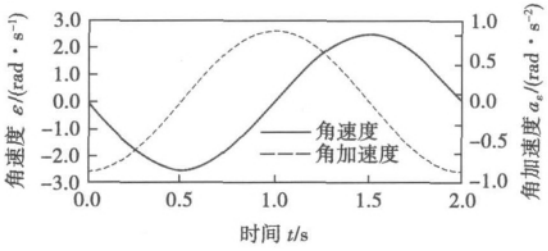

图 7 肩与臂关节角速度及角加速度曲线

Fig. 7 Curve of angular velocity and angular acceleration for arm and shoulder joint

明躯干绕基座转动为匀速转动，正、负峰值均为 180°，说明躯干正好绕机座转动一周，符合实际需要.

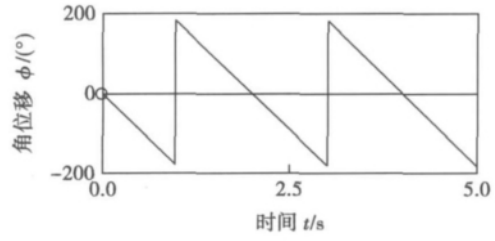

图 8 躯干与基座角位移曲线

Fig. 8 Angular displacement for trunk and base joint

5.3 理论计算与仿真分析结果比对

将建模时的数据，$l_1 = 0.6$ m，$l_2 = 0.4$ m，$l_3 = 0.8$ m，$l_4 = 0.1$ m，$l_5 = 0.6$ m；$\theta_1 = 90°$，$\theta_2 = 60°$，其它数据为零，代入理论公式(5)，得

$$x = 0.6\cos 90° - 0.4\cos 60° - 0.8\cos 0° - 0.1\cos 0° - 0.1\cos 0° = -1.2$$

$$y = 0.6\sin 90° + 0.4\sin 60° + 0.8\sin 0° + 0.1\sin 0° + 0.1\sin 0° = 0.95$$

与仿真结果图 4 中所示非常接近，说明理论与仿真分析一致，仿真结果正确合理.

6 结 论

(1) 对比理论分析和仿真结果，可以看出焊接机器人按照设计预定的轨迹运动，而且机器人运动连续、平稳、运动性能良好，各构件没有产生干涉现象，各个关节角位移、角速度、角加速度连续、无突变连续，表明运动过程平稳、无剧烈的抖动现象、无较大冲击，可以保证焊接质量.

(2) 文中所述方法为焊接机器人的后续设计与制造提供了依据，对于其它类似的机器人轨迹模拟和仿真分析也具有一定的参考意义.

参考文献:

[1] 崔 鲲，戴 明. 冗余自由度弧焊机器人路径自主规划的优化控制[J]. 焊接学报，1998，19(3)：190－196.
Cui Kun，Dai Ming. Autonomous path planning for arc welding robot with redundant degree of freedom [J]. Transactions of the China Welding Institution，1998，19(3)：190－196.

[2] 黄 真，赵永生，赵铁石. 高等空间机构学[M]. 北京：高等教育出版社，2006.

[3] 于靖军，刘辛军，丁希仑. 机器人机构学的数学基础[M]. 北京：机械工业出版社，2009.

[4] 李增刚. ADAMS 入门详解与实例[M]. 北京：国防工业出版社，2008.

[5] 唐新华，Paul Drews. 机器人三维可视化离线编程和仿真系统[J]. 焊接学报，2005，26(2)：64－68.
Tang Xinhua，Paul Drews. 3D-visualized offline-programming and simulation system for industrial rbots [J]. Tromsuctions of the China Welding Institution，2005，26(2)：64－68.

[6] 陈德民，槐创锋. 精通 ADAMS2005/2007 虚拟样机技术[M]. 北京：化学工业出版社，2010.

作者简介：王 玉，女，1969 年出生，硕士，副教授，教研室主任，中国工程图学学会职业技术研究与应用工作委员会委员. 主要从事机械仿真分析与设计方面的研究. 发表论文 20 余篇. Email：hb3321@126.com.

factor, the influence of strength mismatching for welded joints with shallow cracks is more significant than those with deep cracks. When the base metal doesn't show yield platform, the cracking driving force increases monotonously with the applied strain. For the base metal with yield platform, the cracking driving force and applied strain relationship presents a stage change for over-matched or welded joint with shallow crack, which caused by that the strain hardening of base metal lags behind the deformation of weld metal.

Key words: strength mismatch; crack driving force; crack tip opening displacement; finite element method

Investigation on microstructure and microhardness of linear friction welded joints of dissimilar titanium alloys

ZHANG Chuanchen[1], HUANG Jihua[1], ZHANG Tiancang[2], JI Yajuan[2] (1. School of Materials Science and Engineering, University of Science and Technology Beijing, Beijing 100083, China; 2. Beijing Aeronautical Manufacturing Technology Research Institute, Beijing 100024, China). pp 97 – 100

Abstract: On the basis of previous welding experiments, the dissimilar titanium alloys TC4/TC17 were welded by linear friction welding and the interface temperature was measured. The joint microstructure and microhardness was analyzed and tested by optical microscope, scanning electronic microscope and microhardness tester, respectively. The results showed that the interface temperature during welding exceeds 1 200 ℃, above β-transformation temperature. Recrystallization happens in the weld zone in the cooling process after welding, which forms a refined needle-like structure. The recrystallized structure of the mixture zone is equiaxed and even spheroidized. In the TMAZ of TC4, the microstructure consists of the elongated α phase and the broken β phase. In the TC17 TMAZ, the α and β phases was elongated and fined. The microhardness results showed that strain-hardening occured in TC4 TMAZ, while TC17 TMAZ was softened near the weld zone and strain-hardening was obvious near the base metal.

Key words: linear friction welding; titanium alloy; microstructure; recrystallization; microharhness

Microstructure and properties of ESD coating on aluminum alloy

GUO Feng, SU Xunjia, LI Ping, HOU Genliang (The 501 Staff of the Second Artillery Engineering University, Xi'an 710025, China). pp 101 – 104

Abstract: Using silicon bronze electrode, 2A12 aluminum alloy surface was strengthened by electrospark deposition process. The microstructure, element distribution and phase structure of deposited coating were analyzed by scanning electron microscopic, energy-dispersive spectrum and X-ray diffractometer, respectively. Furthermore, the microhardness distribution and wear resistance of deposition coating were studied by microhardness tester and abrasion tester, respectively. The results show that the deposition coating has an average thickness of about 30 μm and forms metallurgical bonding with the substrate. The deposition coating is mainly composed of Cu-Al intermetallic compounds, its microhardness can reach 578 HV. Compared with the 2A12 aluminum alloy substrate, the wearing volume loss of deposition coating is less than one fifth of the substrate. The surface performance of 2A12 aluminum alloy is improved obviously.

Key words: electrospark deposition; aluminum alloy; microhardness; wear resistance

Investigation on Pop-in phenomenon and its causes in CTOD test for weld metal

WU Shipin, WANG Dongpo, DENG Caiyan, WANG Ying (Tianjin Key Laboratory of Advanced Joining Technology, Tianjin University, Tianjin 300072, China). pp 105 – 108

Abstract: CTOD tests were carried out for submerged arc weld seam of offshore platform structures based on BS7448 standard, and the Pop-in phenomenon was assessed and CTOD values were calculated. The results show that when Pop-in phenomenon appears, the fracture toughness CTOD (δ_{Pop}) will decrease several to more than ten times than that without considering Pop-in phenomenon. The research shows that Pop-in phenomenon is mainly due to local brittleness in crack tip, which can be caused by the slag inclusion in local zone of crack tip or the precipitation net in the grain boundary appeared in microstructure of local crack tip. In addition, when there were massive FSP (ferrite side plate) and B (bainite) in one seam of multi-pass weld, local brittleness was easily to occur and lead to Pop-in phenomenon if the crack tip just located in the zone of brittle microstructure and its propagation direction was parallel to the growth direction of brittle microstructure.

Key words: crack tip opening displacement; submerged arc welding; Pop-in phenomenon; local brittleness; fracture toughness

Research on welding robot trajectory and motion simulation based on virtual prototype technology

WANG Yu[1], WANG Qihua[2], ZHAO Jianguang[3], ZHANG Zhaolong[1] (1. Department of Mechanical Engineering, Hebei Institute of Mechanical and Electronical Technology, Xingtai 054048, China; 2. School of Manufacturing Science & Engineering, Sichuan University, Chengdu 610065, China; 3. Department of Electronical Engineering, Hebei Institute of Mechanical and Electronical Technology, Xingtai 054048, China). pp 109 – 112

Abstract: According to the characteristics of it's structure, a simplified model based on kinematics positive direction analysis of welding robot was presented, with the method of Denavit-Hartenber (D-H) matrix, it then solved the mathematical model of the end pose of the welding robot and the description of welding robot's orientation and posture. With the software ADAMS, the motion simulation model of the welding robot was built up, the simulation trajectory of the end of model was obtained, and which was compared with the solution of the mathematical model to verify the accuracy and reliability of the mathematical model. With the simulation analysis of welding robot, the changes of kinematic parameters of the robot's joints were measured and studied, to provide the basis for subsequent design and manufacture of welding robot. It is very meaningful to set the welding position exactly, to ensure the welding quality and to reduce waster.

Key words: welding robot; motion simulation model; degree of freedom; ADAMS; kinematic simulation